ARCHIVES OF CIVIL AND MECHANICAL ENGINEERING 18 (2018) 479–489

Available online at www.sciencedirect.com

ScienceDirect

journal homepage: http://www.elsevier.com/locate/acme

Original Research Article

Novel non-invasive seismic upgradation strategies for gravity load designed exterior beam-column joints

Ashok Kumar Kanchana Devi [a,b,*], Ramajaneyulu Karusala [a,b,1], Mayank Tripathi [b], Saptarshi Sasmal [a,b,2]

[a] CSIR-Structural Engineering Research Centre, Chennai 600113, Tamil Nadu, India
[b] Academy of Scientific and Innovative Research (AcSIR), Taramani, Chennai 600113, Tamil Nadu, India

ARTICLE INFO

Article history:
Received 15 February 2017
Accepted 23 August 2017
Available online

Keywords:
Beam-column joint
Upgradation
Energy dissipation
Strength degradation
Reverse cyclic

ABSTRACT

Existing gravity load designed (GLD) structures are vulnerable to seismic event due to their inherent weaknesses. The present study, focuses on the development of non-invasive and feasible strategies for seismic upgradation of these non-seismically designed structures. Three novel schemes, namely (i) single haunch upgradation scheme (U1), (ii) straight bar upgradation scheme (U2) and (iii) simple angle upgradation scheme (U3) are proposed for seismic upgradation of GLD specimens. The efficacy and effectiveness of these upgradation schemes are evaluated by conducting the reverse cyclic load tests on control and upgraded GLD exterior beam-column sub-assemblages. The performance of the upgraded specimens is compared with that of the control GLD beam-column sub-assemblage, in terms of load–displacement hystereses, energy dissipation capacities and global strength degradation behaviour. Tremendous improvement in the energy dissipation capacity to the tune of 2.63, 2.83 and 1.54 times the energy dissipated by the control GLD specimen is observed in single haunch upgraded specimens, straight bar upgraded specimen and simple angle upgraded specimen respectively. The specimen with single haunch upgradation performed much better compared to the GLD specimens upgraded with the other two schemes, by preventing the brittle anchorage failure, delaying the joint shear damage and redirecting the damage partially towards the beam.

1. Introduction

Prior to the introduction of modern seismic codes, the structures were designed to cater for gravity loads, i.e. the self-weight of the structural components and possible imposed vertical load acting on the structure. Hence, structural components of GLD structures do not have adequate reinforcement to cater for the seismic forces. Further, joints of GLD buildings lack confinement, transverse reinforcement

* Corresponding author at: Advanced Concrete Testing and Evaluation Laboratory, CSIR-SERC, Taramani, Chennai 600113, Tamil Nadu, India.
E-mail addresses: kanchana@serc.res.in (A.K. Kanchana Devi), rams@serc.res.in (R. Karusala), tripathimayank93@gmail.com (M. Tripathi), saptarshi@serc.res.in (S. Sasmal).

[1] Address: Advanced Concrete Testing and Evaluation Laboratory, CSIR-SERC, Taramani, Chennai 600113, Tamil Nadu, India.
[2] Address: Bridge Engineering, CSIR-SERC, Taramani, Chennai 600113, Tamil Nadu, India.

http://dx.doi.org/10.1016/j.acme.2017.08.005
1644-9665/

and hence possess inadequate shear resistance. Insufficient anchorage of the beam bottom reinforcement of GLD frames leads to the anchorage failure or brittle bond failure under seismic loading, leading to huge strength degradation. Particularly, exterior joints of GLD building are more vulnerable and critical as they do not possess a robust force transfer mechanism. Hence, seismic upgradation of beam-column sub-assemblages of GLD buildings has to be addressed immediately to prevent collapse of the existing GLD buildings under seismic excitations.

Plenty of studies were reported in the literature on upgradation/retrofitting of non-seismically designed beam-column sub-assemblages using jacketing, near surface mounting technique, fibre reinforced polymer (FRP) wrapping, haunch retrofitting, joint enlargement, etc. Seismic retrofitting/upgradation using jacketing is a decade old method. Upgradation or retrofitting of beam-column joints was carried out by reinforced concrete jacketing [1,2], steel jacketing [3,4], high performance fibre reinforced concrete jacketing [5–7], hybrid jacketing i.e. combination retrofit strategies with jacketing [8,9]. Seismic retrofit/upgradation using fibre reinforced polymer wrapping or anchoring or the combination of the both was proved as an effective technique by El-Amoury and Ghobarah [10], Prota et al. [11], Akguzel and Pampanin [12], Sezen [13], and Realfonzo et al. [14]. Furthermore, Vecchio et al. [15] proposed a new strength capacity model to predict the increase in strength provided by FRP systems in the seismic retrofit of poorly detailed corner joints. The accuracy of the proposed model was assessed by comparing the predicted results of the model with large database of experimental tests. Near surface mounting technique is frequently complemented with the FRP retrofit schemes for the effective retrofitting of the parent member. Prota et al. [11] upgraded under-designed interior beam-column joints by combined use of externally bonded fibre-reinforced polymer (FRP) laminates and near surface-mounted (NSM) FRP bars. The upgradation scheme involves different combinations of FRP laminates around column/beam with or without NSM bars.

The concept of haunch retrofit solution was perceived by Yu et al. [16] for steel moment resting frames in view of significant failure of welds during Northridge earthquake. The concept of this haunch strengthening scheme was adopted and implemented for GLD RC structures by Pampanin et al. [17,18]. Genesio et al. [19] and Sharma et al. [20] investigated the performance of haunch system connected to the beam and column through post-installed anchors. This was termed as fully fastened haunch retrofit system. Sharbatdar et al. [21] retrofitted the damaged exterior beam-column joints using steel prop and curb by providing two each at the top and bottom faces of the beam and connecting the beam and the column. It was reported that there was a significant increase in ultimate load and decrease in degradation of retrofitted damaged joints. Further, they reported that the energy absorption was enhanced and the cracks were minimized due to retrofitting. Shafaei et al. [22] proposed an innovative seismic retrofit scheme for strengthening of non-seismically detailed beam column joints by the use of prestressed steel angle sections. It was found from their experimental study that with proper implementation of strategy, the plastic hinge can be relocated into the beam region. Campione et al. [23] used steel cages for strengthening of the exterior beam-column sub-assemblages and proposed a simplified analytical model that can be used for pushover analysis. The results obtained from their study highlighted the effectiveness of the external steel cage as strengthening system, which increases the flexural strength and facilitate to shift the failure mode from the column to the beam.

Most of the reported works were successful in achieving the desired seismic performance level either completely or partially. However, when it comes to implementation on the existing deficient structure, almost it is very difficult to implement the reported retrofitting schemes as they need to access column, beams and joints from all the four sides. The expediency of any retrofitting scheme could be fully exploited only when it is feasible to practice. Unless the retrofitting scheme is implementable, it would become useless even though the scheme is so robust. For this reason, in the present study emphasis has been laid for the development of implementable novel seismic upgradation scheme for GLD structures. In an existing structure, the bottom portion of the floor beam and adjacent column would be easily accessible which is the key for the development of upgradation strategies in the present study. The GLD beam-column joints are susceptible to sudden anchorage failure under load reversals and hence require systematic seismic upgradation. For this reason, the primary aim of the present work is to avoid anchorage failure of beam bottom reinforcement bars of GLD structure and delaying the joint damage as far as possible under seismic loading. The seismic upgradation of the exterior beam-column sub-assemblages are carried out using three novel schemes, namely (i) single haunch upgradation scheme (U1), (ii) straight bar upgradation scheme (U2) and (iii) simple angle upgradation scheme (U3). The first two upgradation schemes provide an alternate force path and thereby reduce the demand on the components of sub-assemblages whereas the third scheme involves strengthening of the beam bottom to prevent brittle anchorage failure of beam bottom reinforcement bars. The efficacy of these novel upgradation schemes is evaluated by conducting reverse cyclic load tests on the retrofitted GLD exterior beam-column sub-assemblages. The performance of the upgraded GLD specimens is compared with the control GLD beam-column sub-assemblage, in terms of load–displacement hystereses, energy dissipation capacities and global strength degradation behaviour.

2. Details of the beam-column sub-assemblage specimens

An exterior beam-column sub-assemblage of a typical three storied RC framed building as shown in Figs. 1(a) and (b) is taken up. The general dimensions of beam-column sub-assemblage are as follows: height of column segment is 3800 mm and length of beam segment is 1700 mm. The cross sectional dimensions adopted for beam and column sections are $300\ \text{mm} \times 400\ \text{mm}$ and $300\ \text{mm} \times 300\ \text{mm}$ respectively, and the reinforcement details of GLD specimen are shown in Fig. 1(c). It is important to mention here that the beam bottom bars in gravity load designed specimen project straight into the joint region. Four such specimens are cast and one of them is

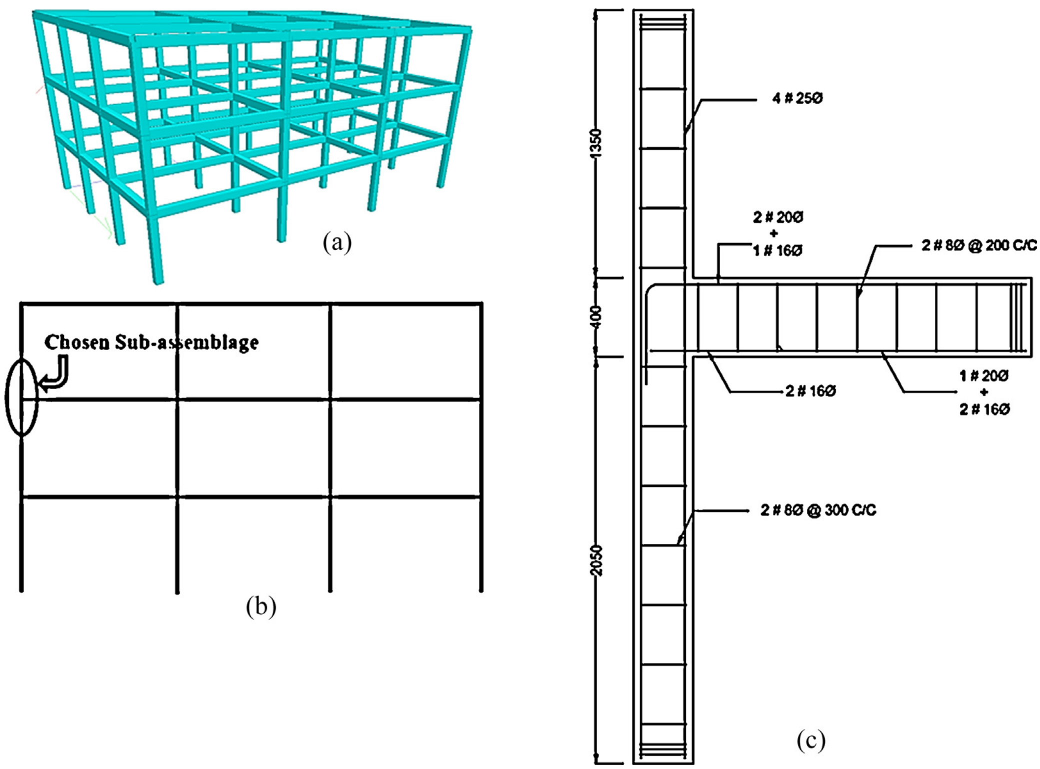

Fig. 1 – (a) Building chosen for study. (b) Chosen typical exterior beam-column sub-assemblage. (c) Details of gravity load specimen (SP1).

control GLD specimen (SP1) and the other three specimens are used for upgradation with three different schemes. The concrete of mix proportions 1:1.695:3.013 with water cement ratio of 0.5 is used for casting the specimens. The specimens are cast and cured for 28 days using wet curing. The concrete cylinders that are cast along with four beam–column sub-assemblages are tested for compressive and split tensile strength and the average strengths are as given in Table 1. The material properties of steel reinforcement used for the study are given in Table 2.

Table 1 – Strength parameters of concrete.

Specimen ID	Average compressive strength (N/mm^2)	Average split tensile strength (N/mm^2)
SP1	41.34	3.7
SP1-U1	38.71	3.29
SP1-U2	37.35	3.52
SP1-U3	38.5	3.22

Table 2 – Material properties of steel reinforcement.

Diameter of reinforcement (mm)	Yield strength of steel (N/mm^2)
8	527
16	520
20	545
25	535

3. Details of upgradation schemes

Three upgradation schemes are proposed in the present study, with the view of implementing in the existing GLD structures without any difficulty. The three schemes are (i) single haunch upgradation scheme (U1), (ii) straight bar upgradation scheme (U2), and (iii) simple angle upgradation scheme (U3).

4. Single haunch upgradation scheme (U1)

For single haunch upgradation scheme (U1), a single steel bracing is introduced between adjacent beam and column segments at the bottom of the beam as shown in Fig. 2(a). The steel haunch bracing consists of 30 mm diameter plain steel rod welded at both of its ends to square bearing plate each of 300 mm × 300 mm × 12 mm. The rod is stiffened by means of the triangular stiffener plate of 150 mm × 150 mm × 6 mm at both ends of the rod as shown in Fig. 2(a). The bearing plates are connected to the faces of beam and column using adhesive anchors (Hilti HAS-E bolts with HVU adhesive) of 20 mm diameter and 170 mm embedment length. The bearing plates are positioned at a distance of 400 mm from the face of the joint to the centre of the plate. The haunch is designed as yielding haunch at load corresponding to the yielding of reinforcement bars at beam top. Hence, the haunch should be capable of resisting the force till the yielding of beam top reinforcement and thereafter sustains the same load. The size of the haunch is arrived to cater for the force that would be

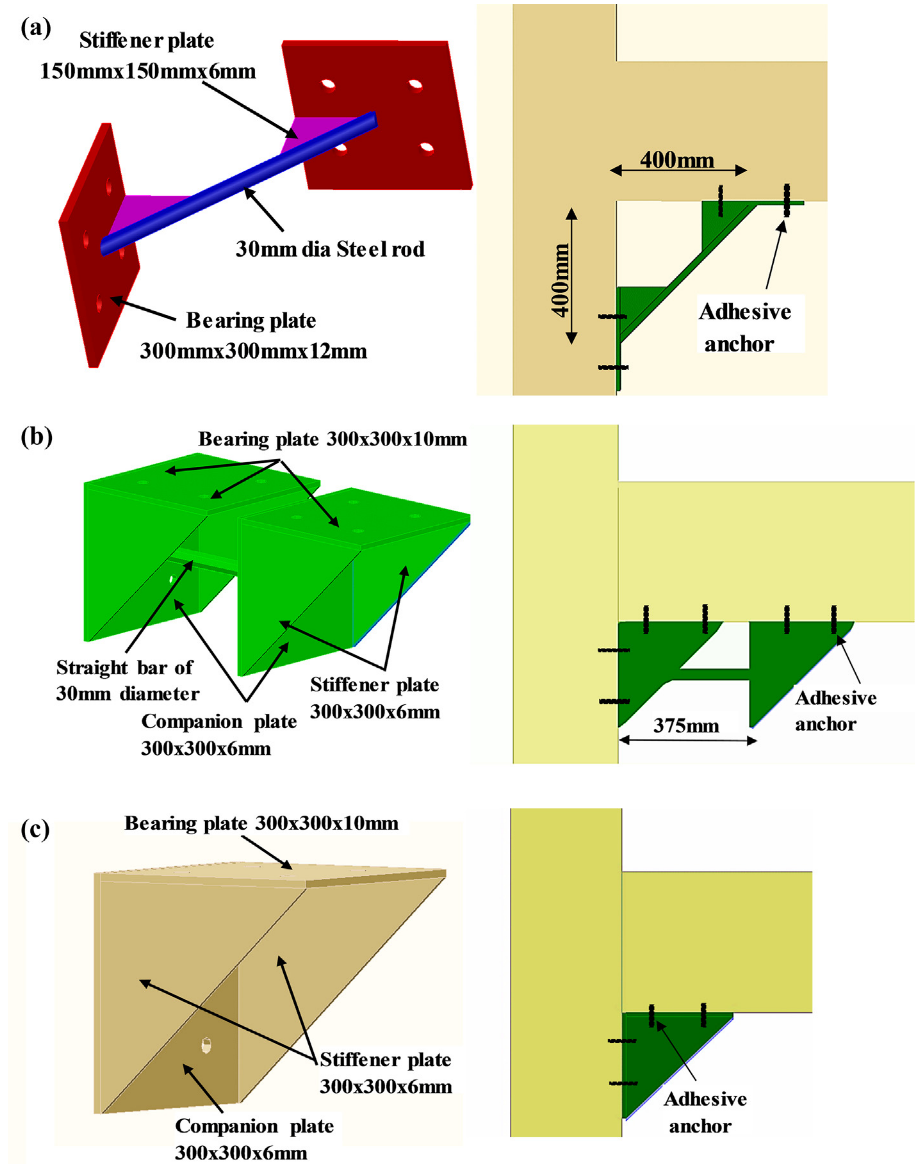

Fig. 2 – (a) Schematic details of single Haunch upgradation scheme (U1). (b) Schematic details of Straight bar upgradation scheme (U2). (c) Schematic details of simple angle upgradation scheme (U3).

directed into the haunch at the yielding of beam top reinforcement. The introduction of haunch produces vertical and horizontal forces at the haunch-beam and haunch-column connection points. The vertical component of the haunch force introduces shear opposite to beam shear (i.e. beam loading) and horizontal component of the haunch force at beam bottom produces a concentrated moment about the beam centre at the location of haunch beam connection in the direction opposite to that due to loading at the beam end. Thus, there would be a reduction in the beam bending moment due to vertical and horizontal components of haunch force. The reduction in the beam bending moment in turn reduces the joint shear, thus the presence of single haunch would improve the load carrying capacity of the upgraded beam-column sub-assemblage and also may tend to delay the joint damage in a much better way compared to control GLD beam-column sub-assemblage. This may also result in the improvement in the energy dissipation capacity locally, thereby improving the global energy dissipation of the upgraded structure which is the most desired aspect from the seismic resistant design point of view. Further, the haunch acts as a partial support and enables the beam bottom bars to develop and prevent the anchorage failure of beam bottom reinforcement bars.

5. Straight bar upgradation scheme (U2)

The straight bar upgradation scheme (U2) consists of introducing the mild steel bar of 30 mm diameter parallel to the beam. The mild steel rod is connected to adjacent beam and column segments by means of the stiffened angles as shown in Fig. 2(b). The bearing plates of size 300 mm × 300 mm × 10 mm are welded to form an angle and this is stiffened on the sides by triangular stiffener plates of size 300 mm × 300 mm × 6 mm. A mild steel straight bar of 30 mm diameter connects the two stiffened angles to form the full assemblage as shown in Fig. 2(b). The straight bar assembly is connected to beam and column segments of beam-column sub-assemblage by means of adhesive anchors (Hilti HAS-E bolts with HVU adhesive) of 20 mm diameter and 170 mm embedment depth. This innovative straight bar upgradation scheme is devised to provide an alternative means to cater to the tensile force at beam bottom and thereby aids in preventing the most brittle anchorage failure of beam bottom reinforcement. The provision of straight bar would improve the load carrying capacity of the beam-column sub-assemblage under positive loading cycles [beam bottom bars under tension] and this in turn results in the improvement in the energy dissipation capacity of the upgraded specimen. Further, it would produce concentrated moment about the centre of the beam in the direction opposite to that caused due to the load at beam tip and thereby reduces the beam moment which in turn reduces the joint shear. The extent of reduction in beam moment and joint shear in this scheme is less when compared to that in the single haunch scheme. Hence, it is expected to improve the load carrying capacity in positive loading cycles and also there would be a slight improvement in load carrying capacity in the negative loading cycles.

6. Simple angle upgradation scheme (U3)

Simple angle upgradation scheme (U3) consists of introducing single stiffened angle underneath the beam and adjacent to the column. The angle is made by welding two plates of size 300 mm × 300 mm × 12 mm. The angle is stiffened on the sides by means of triangular stiffener plates of size 300 mm × 300 mm × 6 mm. Typical simple stiffened angle upgradation scheme is as shown in the Fig. 2(c). The angle is connected to beam and column segments of beam-column sub-assemblage by means of the post-installed adhesive anchors of 20 mm diameter and 170 mm embedment depth as shown in Fig. 2c. The beam bottom is strengthened by single stiffened angle with the view of preventing the anchorage failure of beam bottom bars and to delay the cracking at the face of the joint. Hence, it is expected to improve the load carrying capacity during the positive cycle of loading and achieve improvement in the energy dissipation capacity. This scheme is tried as it is the simplest and would be at the lower limit compared to single haunch and straight bar upgradation schemes. Further, this is the easiest of all the upgradation schemes.

7. Set up and instrumentation adopted for experimental investigations

The test specimens are instrumented with LVDTs (linear variable displacement transducers), which were mounted on the joint surface as well as on the beam and the column segments to measure deflections along the length of beam and column segments and to evaluate the rotation of the joint. The strain gauges are affixed on the reinforcement bars of the beam, columns and stirrups in the disturbed region. The test setup is arranged on the test floor so that the beam-column joint is positioned horizontally parallel to the test floor and the cyclic load is applied in the plane of the test floor. The test set-up, positioning of test specimen and instrumentation adopted is shown in Fig. 3. An axial load of 300 kN is applied to the column by a hydraulic jack at one end of the column against the reaction block at the other end. The level of axial load (about 10% of the strength) in the column is arrived by carrying out an analysis of the global system of the three storey three-bay building. The lateral load is applied on the beam tip in a displacement control mode using 25 T actuator, according to the load history shown in Fig. 4. Reverse cyclic load is applied in terms of drift ratio (%) of the component where the drift ratio is calculated as per Eq. (1).

$$\text{Drift ratio } (\%) = \left(\frac{\Delta l}{l_b}\right) \times 100 \tag{1}$$

where, Δl and l_b are the applied displacement at the beam tip and the length of the beam from column face to the point of application of the displacement increment respectively. Three complete cycles are applied for each drift increment. Reverse cyclic displacements of equal magnitude are applied to the

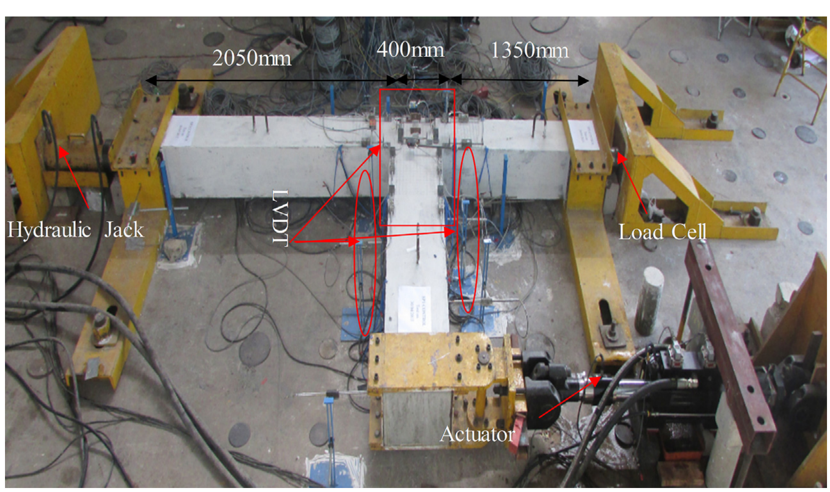

Fig. 3 – Set up and instrumentation adopted for experimental investigation.

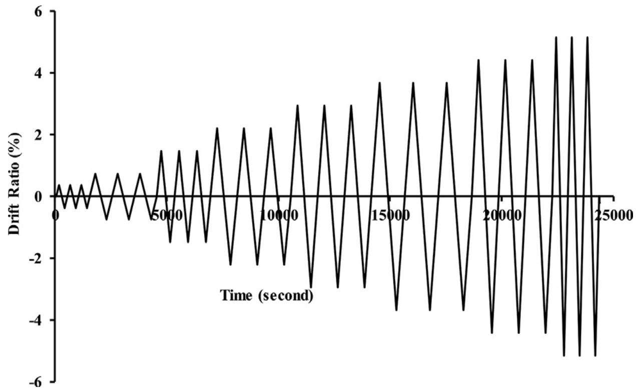

Fig. 4 – Displacement history used in the experimental investigations.

specimens, where positive drift produces tension in the beam bottom and negative drift produces tension in beam top. The drift cycles are incremented till the failure of the specimen.

Experimental investigations are carried out on all the four specimens, viz., control GLD specimen (SP1), GLD specimen upgraded with single haunch upgradation scheme (SP1-U1), GLD specimen upgraded with straight bar upgradation scheme (SP1-U2) and GLD specimen upgraded with simple angle upgradation scheme (SP1-U3). The data acquired during experimental investigations on all the specimens are processed in order to assess their seismic performance.

8. Results and discussion

Upon the application of reverse cyclic loading in the displacement control mode, cracks are developed initially on the beam in all the four specimens till the drift ratio of 0.735%. Crack patterns observed in all the specimens during positive cycle at drift ratios of 1.47% (at anchorage failure of SP1) and 2.94% (final stage of SP1) are shown in Fig. 5. In control GLD specimen SP1, the damage progression happened in the form of prominent joint crack at the face of the column due to anchorage failure of beam bottom reinforcement during the positive cycle of 1.47% drift ratio. Whereas at same drift ratio the GLD specimen with single haunch upgradation (SP1-U1) developed a distinct crack in the beam at the location of haunch during the positive loading cycles. This crack got widened with the drift increment as long as the haunch is effective. The GLD specimen upgraded with straight bar (SP1-U2), developed cracks in the beam at the drift ratio of +1.47%, approximately at distance D/2 from the face of the joint, where D is depth of the beam. Further, the diagonal shear cracks are also appeared at the same drift cycle. With the further drift increment, the damage progression happened in the form of widening of diagonal shear cracks. During positive drift cycles of 1.47%, the GLD specimen upgraded with simple angle (SP1-U3) developed flexural crack approximately at 50 mm from the face of the joint and fine hair–line diagonal shear cracks appeared in the joint region. With the further drift increment, the cracks are developed in the beam at the face of the angle-beam connection as the presence of angle prevented the widening of the joint crack and allowed the crack development in beam beyond the location of angle. Thus, during the positive cycle of loading the anchorage failure is avoided and yielding of reinforcement is observed in the case of upgraded specimens SP1-U1 and SP1-U2. In the case of upgraded specimen SP1-U3, the anchorage failure happened at larger drift ratio, i.e. at 2.21% as against 1.47% in the case of control GLD specimen SP1.

Crack patterns observed in all the four specimens during negative cycles at drift ratios of −1.47% and −2.94%, are shown

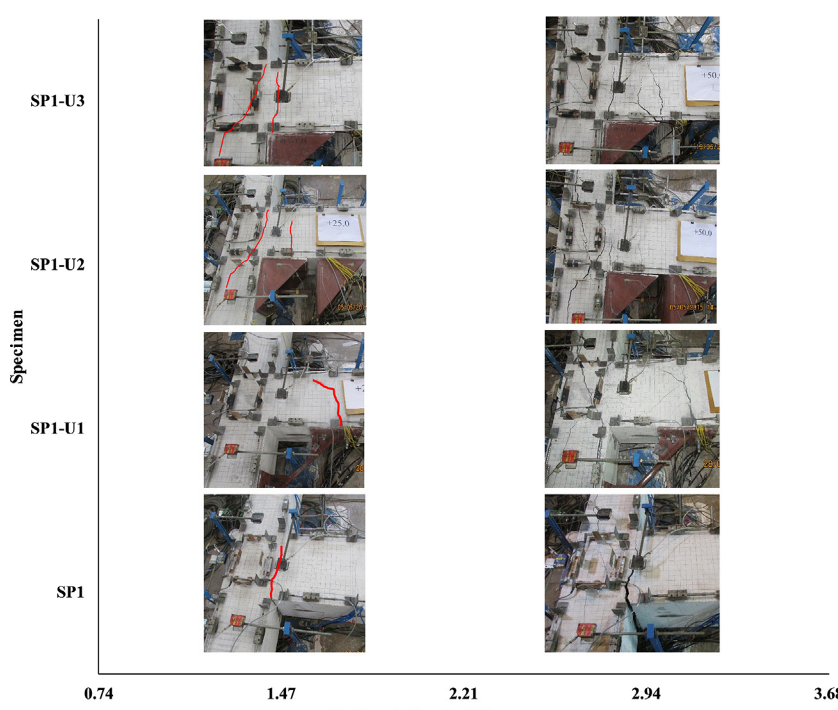

Fig. 5 – Crack patterns observed in control and upgraded GLD specimens during positive drift cycles.

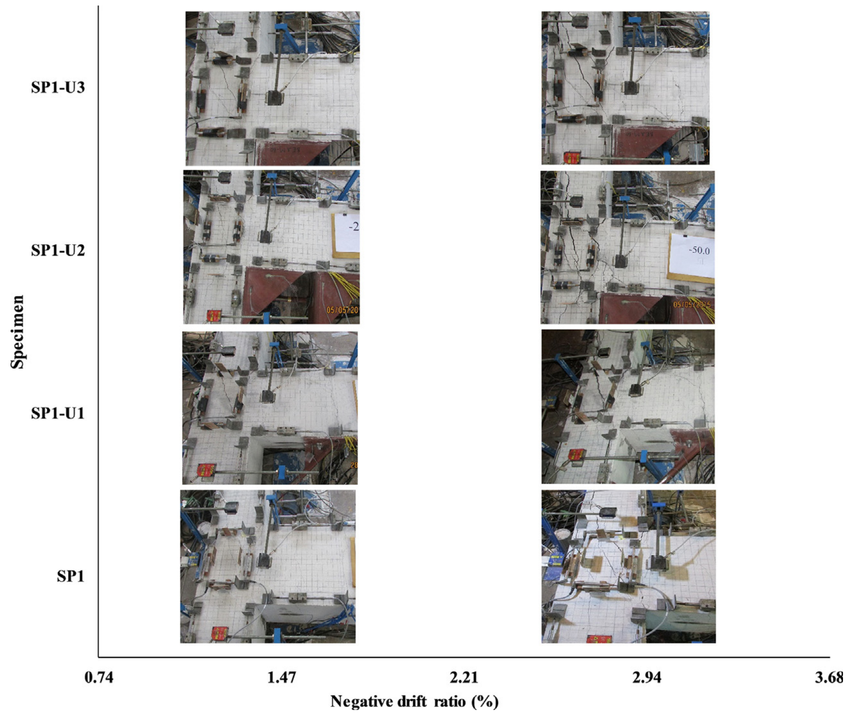

Fig. 6 – Crack patterns observed in control and upgraded GLD specimens during negative drift cycles.

in Fig. 6. During the negative cycles, all the specimens showed similar behaviour, i.e. the diagonal shear cracks appeared at the drift ratio of −1.47% and also yielding of reinforcement commenced at the same drift cycle. Thereafter, the damage progression had happened in the form of joint shear cracks and degradation in load displacement behaviour. The single haunch upgraded GLD specimen SP-U1 and the specimen upgraded with straight bar SP1-U2 carried higher load compared to that of the control GLD specimen SP1. There is a delay in the shear failure in the case of these two upgraded specimens, whereas the simple angle upgraded GLD specimen SP1-U3 behaved similar to that of the control GLD specimen.

9. Load displacement behaviour of control and upgraded GLD specimens

The load–displacement hysteresis curves obtained for all the four specimens are depicted in Fig. 7. The control GLD specimen SP1 being seismically deficient exhibited poor hysteretic performance. At drift ratio of +1.47%, sudden load drop is observed due to anchorage failure of beam bottom reinforcement bars. With subsequent drift increments, the load dropped drastically from the maximum load of 39 kN to 14 kN (Load corresponding to third cycle of 50 mm i.e. drift ratio 2.94%). During the negative cycle, the yielding of beam top reinforcement commenced at drift ratio of −1.47%, which is accompanied by diagonal crack formation in the joint. Further, the specimen exhibited global strength degradation at the drift ratio of 2.2% due to joint shear failure. The maximum load carried by the specimen during positive and negative cycles are 39 kN and 85 kN respectively. This non-uniform load carrying capacity is owing to the unequal areas of reinforcement steel at beam top and bottom.

In single haunch upgraded GLD specimen SP1-U1, introduction of haunch below floor beam produces vertical and horizontal forces at haunch-beam and haunch-column connection. This in turn reduces the beam moment at the joint which ultimately reduces the joint shear demand. Furthermore, the haunch acts as a partial support, thereby facilitating the development of beam bottom reinforcement bars and thus the anchorage failure of the beam bottom bars is prevented at a drift ratio of +1.47% in the case of upgraded GLD specimen SP1-U1. This could also be witnessed from load–displacement curve where sudden load drop is not observed unlike in the control GLD specimen SP1. Further in the negative cycle, due to the reduction of shear demand on the joint there is improvement in the load carrying capacity of SP1-U1 specimen compared to that of control GLD specimen SP1. The maximum load carried by upgraded specimen SP1-U1 during positive and negative displacement cycles are 69 kN and 110 kN respectively. The load begins to drop in the positive cycle after the drift ratio of 2.2%. The yielding of beam reinforcement was observed during both positive and negative displacement cycles in the upgraded GLD specimen SP1-U1. During negative cycle, beyond the drift ratio of −2.2%; the global strength degradation begins due to the joint shear failure. Even though, the joint shear failure could not be avoided in the negative cycles, the brittle anchorage failure of beam bottom reinforcement could be prevented and the damage is partially redirected towards the beam in the positive cycles. As the specimen carried more load than that of the control GLD specimen SP1 during the negative cycle, it may be concluded that joint shear damage is delayed in SP1-U1 when compared

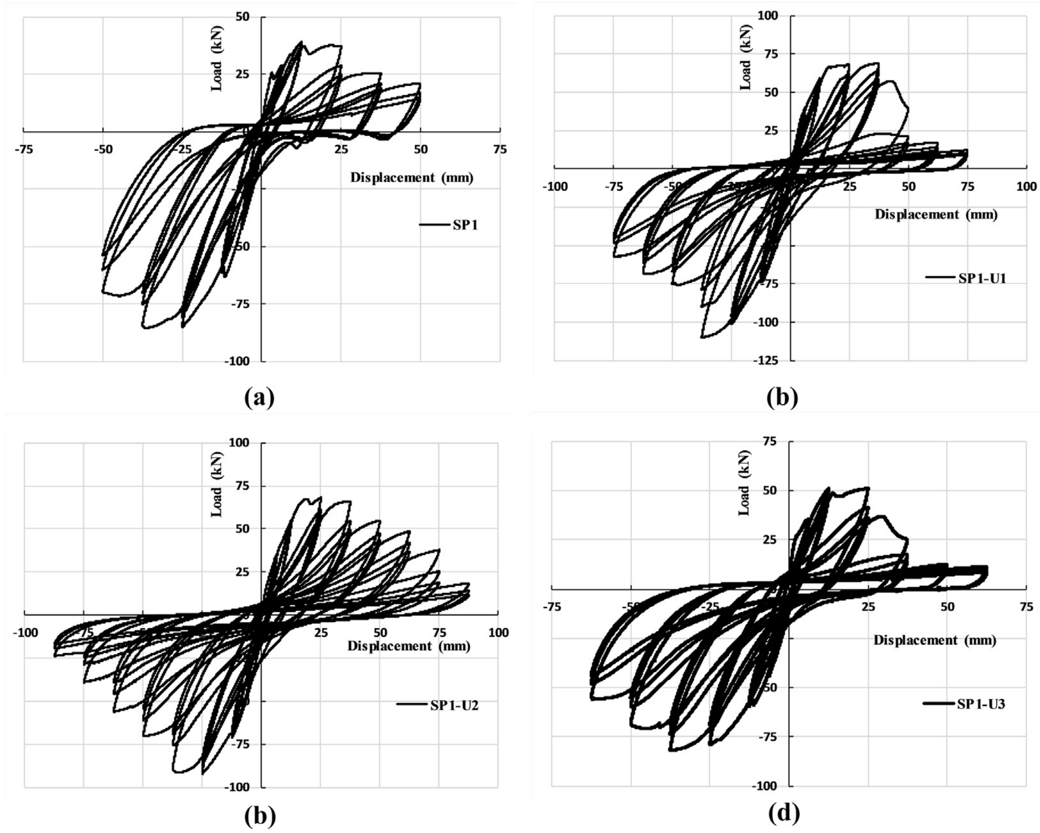

Fig. 7 – Load–displacement hysteresis curves of control and upgraded GLD specimens.

to SP1. Thus, the single haunch upgradation scheme with the yielding haunch in compression would be the better candidate for the structures that are susceptible to moderate seismic risk.

In straight bar, upgraded GLD specimen SP1-U2, the presence of straight bar introduces moment opposite to that of beam moment and thereby reducing the joint shear demand to some extent but less effective than the single haunch upgraded specimen SP1-U1. Moreover, addition of straight bar parallel to the beam reinforcement provides an alternate means to take tensile force at beam bottom and prevents the anchorage failure of beam bottom reinforcement bars. At drift ratio of +1.47%, anchorage failure of beam bottom bars is not observed during the positive cycle. The specimen exhibited uniform strength degradation during the positive cycle after the drift ratio of +2.2%. During the negative cycles, the GLD specimen upgraded specimen with straight bar (SP1-U2) exhibited the behaviour similar to that of the SP1-U1. The specimen carried slightly higher load in negative cycle compared to the control GLD specimen (SP1) and exhibited joint shear failure in the subsequent drift increments. The maximum load carried by the specimen SP1-U2 during the positive and negative displacement cycles is found to be 68 kN and 92 kN respectively. Thus, in SP1-U2, the most brittle anchorage failure of the beam bottom bars is avoided and the upgraded specimen exhibited much better hysteretic performance when compared to SP1 in terms of load carrying capacity and delaying the joint shear damage to some extent but not as effective as SP1-U1.

The upgradation of GLD specimen using simple angle is carried out with the view of preventing the beam anchorage failure. Even though, it is well known that both mechanisms, viz., horizontal and vertical mechanisms of beam moment reduction at joint are absent in simple angle scheme, it is tried as it would prevent opening of the joint and the anchorage failure of beam bottom reinforcement. The introduction of simple angle improves the load carrying capacity slightly during the positive cycle, whereas during the negative cycle there is a slight reduction in load carrying capacity compared to that of SP1. The anchorage failure of beam bottom reinforcement is delayed and occurred at the drift ratio of 2.2% instead of drift ratio of 1.47% (as noticed in control GLD specimen SP1). The maximum load carried by SP1-U3 during the positive and negative cycles are found to be 51 kN and 82 kN respectively. The behaviour of SP1-U3 is similar to that of the control GLD specimen (SP1), except that there is improvement in the load carrying capacity during the positive cycle and anchorage failure of beam bottom bars is delayed due to simple angle upgradation. It is very clear that strengthening of GLD specimen using simple angle at the beam bottom did not exhibit the desired performance level as it could not provide an alternate force path to the system for redirecting the damage towards the beam. However, the performance of SP1-U3 is also better than that of SP1.

The load displacement envelopes obtained for all the four specimens are shown in Fig. 8. From the load displacement envelopes, it could be observed that the upgraded GLD

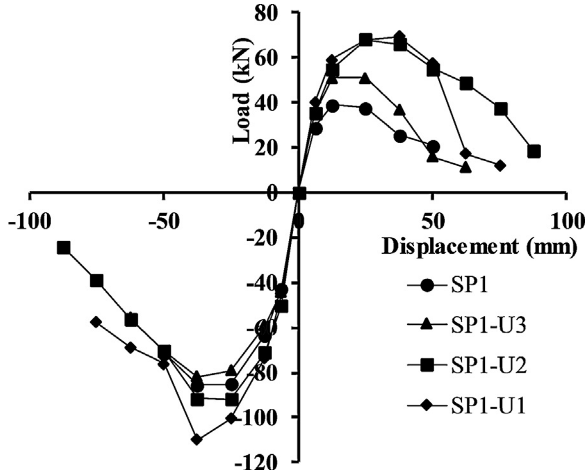

Fig. 8 – Load–displacement envelopes of control and upgraded GLD specimens.

specimens SP1-U1 and SP1-U2 showed similar behaviour during the positive cycles. The maximum load carried by the upgraded GLD specimens SP1-U1, SP1-U2 and SP1-U3 during positive cycles are 77%, 74%, 30%, respectively higher than the maximum load carried by control GLD specimen SP1. A tremendous improvement in the load carrying capacity observed during the positive cycle of loading in SP1-U1 and SP1-U2 is due to the prevention of anchorage failure of beam bottom reinforcement bars. The maximum load carried during negative cycles of upgraded specimens SP1-U1 and SP1-U2 are 28% and 7% higher than that of control GLD specimen SP1 whereas maximum load carried by upgraded GLD specimen SP1-U3 is 4% lower than that of SP1. The improvement in load carrying capacity by upgraded GLD specimens SP1-U1 and SP1-U2 is owing to the reduction of joint shear demand. From the load envelope, it is found that the specimen SP1-U2 showed uniformly degrading behaviour when compared to that of SP1-U1. The specimen SP1-U1 carried higher load when compared to SP1-U2 during both positive and negative cycles. Specimen SP1-U3 had load–displacement envelope similar to that of the control GLD specimen SP1 but proved that even the simple angle strengthening at beam bottom could able to delay the anchorage failure of beam bottom reinforcement bars and could be able to carry 30% more load compared to that of control GLD specimen SP1 during the positive cycles.

The upgradation schemes SP1-U1 and SP1-U2 showed promising hysteretic behaviour with the improved load carrying capacity in both positive and negative cycles. Further, both upgraded specimens sustained larger deformation and exhibited better hysteretic behaviour when compared to the control GLD specimen (SP1). Particularly, the single haunch upgraded GLD specimen SP1-U1 showed a far better performance by preventing anchorage failure, delaying joint failure and succeeding in partially redirecting the damage to the beam. Furthermore, the straight bar upgraded GLD specimen SP1-U2 avoided the brittle anchorage failure of the beam bottom reinforcement bars and exhibited uniformly degrading hysteretic performance. Even though simple angle upgradation scheme is simple and straightforward to implement, it is not sufficient to prevent anchorage failure of beam bottom bars, but succeeded in shifting the anchorage failure to higher drift ratio (From 1.4% in SP1 to 2.2% in SP1-U3). Under moderate earthquake, higher strength of structure is required, so that the structure could resist seismic forces with little repairable damage or without any damage. Hence, under those scenarios upgradation schemes SP1-U1 and SP1-U2 are suitable candidates for seismic upgradation or strengthening of GLD specimens. However, the role of simple angle upgradation cannot be simply ignored in view of its easiest implementability.

10. Energy dissipation

Energy dissipation is one of the key seismic performance parameters as the structure has to dissipate the energy imparted to it during the earthquake. This could be achieved only if the individual sub-assemblages have capability to dissipate energy locally and thus leading to improved overall global behaviour. The cumulative energy dissipated by all the four specimens are shown in Fig. 9. Till the elastic cycles, i.e. up to the drift ratio of 0.737%, all the specimens dissipated same energy. After the drift ratio of 1.47%, the energy dissipated by SP1-U1 is higher than the energy dissipated by SP1-U2 in all drift cycles. At drift ratio of 2.94% (i.e. the maximum drift sustained by control GLD specimen SP1), the cumulative energy dissipated up to 2.94% drift ratio by the upgraded GLD specimens SP1-U1, SP1-U2 and SP1-U3 is 58%, 40% and 15% higher than that of control GLD specimen SP1. The total cumulative energy dissipated by SP1, SP1-U1, SP1-U2, and SP1-U3 are found to be 11.65 kNm, 30.63 kNm, 32.96 kNm, 18 kNm respectively. The total cumulative energy dissipated by SP1-U1, SP1-U2 and SP1-U3 are 2.62, 2.83 and 1.54 times that of the cumulative energy dissipated by SP1. A tremendous improvement in the energy dissipation capacity is observed in the case of upgraded GLD specimens SP1-U1 and SP1-U2. The prevention of beam anchorage failure of beam bottom bars improved the energy dissipation of the GLD specimens drastically. A simple shifting of the anchorage failure of the beam bottom bars from drift ratio of 1.47% to 2.2% in the specimen SP1-U3, increased the energy dissipation by 54% compared to that of SP1. Thus, for GLD specimens with straight bar anchorages, the

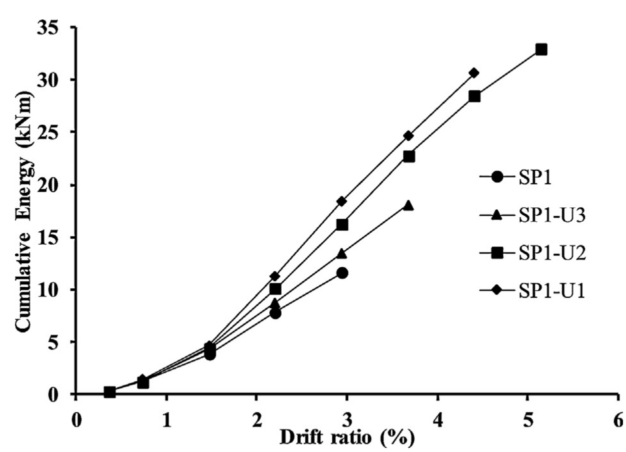

Fig. 9 – Cumulative energy dissipation of control and upgraded GLD specimens.

avoiding or shifting of the anchorage failure would result in the tremendous improvement in the energy dissipation, which is one of the most required aspects for the seismic resist design of the structures. This clearly demonstrates the efficacy of the seismic upgradation strategies proposed in the present study for the GLD structures.

11. Global strength degradation

The strength degradation at first cycle of each drift level with the drift increment is plotted in Fig. 10. For specimen SP1, the strength degradation begins at the drift ratio of +0.735% and −1.47% in the positive and negative cycles respectively. For upgraded GLD specimens SP1-U2 and SP1-U3, the strength degradation begins at the drift ratio of 1.47% in both positive and negative cycles. Even though for specimen SP1-U2, the strength degradation begins at the drift ratio of 1.47%, the degradation at the drift ratio of 2.2% is small and found to be 3% and 0.25% in the positive and negative drift cycles respectively. The specimen SP1-U1 showed superior performance among all the four specimens. The strength degradation in SP1-U1 occurred at the drift ratio of 2.2% in both positive and negative drift cycles. During negative cycle, at drift ratio of −2.94%, the strength degradation of the SP1, SP1-U1, SP1-U2 and SP1-U3 is found to be 16%, 30%, 23%, 13% respectively though the strength degradation percentages are higher in the case of upgraded specimen (SP1-U1 and SP1-U2) the loads carried by the specimens are almost equal (i.e. load dropped from the maximum load of 85 kN to 71 kN, from 109 to 76 kN and from 92 kN to 70KN in SP1, SP1-U1 and SP1-U2 respectively). This is due to the partial reduction of joint demand and the load drop from the improved load carrying capacity to the capacity corresponding to degraded joint strength in the case of upgraded GLD specimens. At drift ratio of +2.94%, the strength degradation of the SP1, SP1-U1, SP1-U2 and SP1-U3 is found to be 46%, 17%, 19%, 69%, respectively. The upgraded specimen SP1-U3 performed similar to that of the control GLD specimen with reference to strength degradation. The upgraded GLD specimens SP1-U1 and SP1-U2 exhibited superior performance in the positive cycle when compared to control GLD specimen SP1.

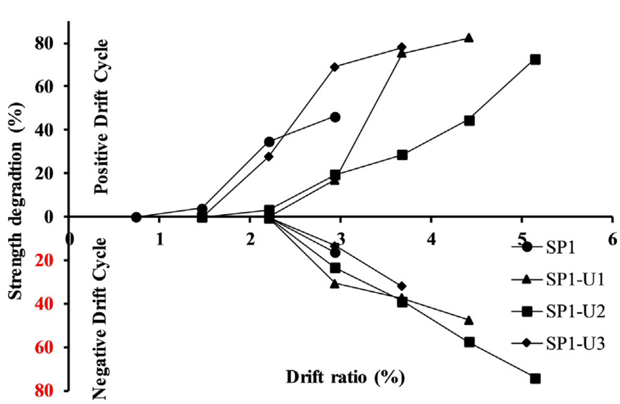

Fig. 10 – Global strength degradation of control and upgraded GLD specimens.

12. Conclusions

The upgradation of typical GLD exterior beam-column sub-assemblage is carried out using three different novel schemes, namely (i) single haunch upgradation scheme, (ii) straight bar upgradation scheme and (iii) simple angle upgradation scheme. The efficacy of the upgradation schemes is evaluated by conducting reverse cyclic load tests on control and three upgraded GLD exterior beam-column sub-assemblages. The single haunch upgraded GLD specimen SP1-U1 and straight bar upgraded specimen SP1-U2 showed superior hysteretic behaviour with the improved load carrying capacity in both positive and negative cycles compared to that of control GLD specimen SP1. Further, both these upgraded specimens could sustain larger drift ratios and exhibited better hysteretic behaviour when compared to the control GLD specimen. The upgraded GLD specimen SP1-U1 showed far superior performance by preventing anchorage failure, delaying joint failure and succeeding in partially redirecting the damage to the beam. The upgraded GLD specimen SP1-U2 avoided the brittle anchorage failure of the beam bottom reinforcement and exhibited the uniformly degrading hysteretic performance. This also demonstrated its fulfilment of the intended purpose of enhanced seismic performance of GLD beam-column sub-assemblages, particularly during positive drift cycles. The simple angle upgraded GLD specimen SP1-U3 could be able to shift the anchorage failure of the beam bottom bars from drift ratio of 1.47% (as noticed in the case of control GLD specimen SP1) to 2.2% even though improvement in load carrying capacity in the positive cycles is less when compared to the other two upgradation specimens (SP1-U1 and SP1-U2). However, the load carried by SP1-U3 in the positive cycles is 30% higher than that of control GLD specimen SP1. A tremendous improvement in the energy dissipation capacity is observed in the case of all the three upgraded specimens compared to control GLD specimen. The cumulative energy dissipated by SP1-U1, SP1-U2 and SP1-U3 are 2.62, 2.83 and 1.54 times the energy dissipated by SP1. Thus, this study provided clear insight into the development of easily implementable seismic strengthening/upgradation strategies for the existing GLD buildings with poor anchorage details. Also, this study demonstrated the efficacy of novel seismic upgradation strategies proposed for GLD structures.

Ethical statement

Authors state that the research was conducted according to ethical standards.

Acknowledgements

The authors express their heartfelt thanks to the support rendered by the staff members of Advanced Concrete Testing and Evaluation Laboratory and Structural Testing Laboratory of CSIR-SERC during the experimental investigations of the beam-column sub-assemblages.

REFERENCES

[1] S.M. Alcocer, J.O. Jirsa, Strength of reinforced concrete frame connections rehabilitated by jacketing, ACI Struct. J. 90 (3) (1993) 249–261.

[2] A.G. Tsonos, Lateral load response of strengthened reinforced concrete beam-to-column joints, ACI Struct. J. 96 (1) (1999) 46–56.

[3] A. Ghobarah, T.S. Aziz, A. Biddah, Rehabilitation of reinforced concrete frame connections using corrugated steel jacketing, ACI Struct. J. 94 (3) (1997) 282–294.

[4] G. Santarsiero, A. Masi, Seismic performance of RC beam–column joints retrofitted with steel dissipation jackets, Eng. Struct. 85 (2015) 95–106.

[5] E. Dogan, N.K. Opara, Seismic retrofit with continuous slurry-infiltrated mat concrete jackets, ACI Struct. J. 100 (6) (2003) 713–722.

[6] M.J. Shannag, S. Barakat, M. Abdul Kareem, Cyclic behaviour of HPFRC-repaired reinforced concrete interior beam-column joints, Mater. Struct. 35 (2002) 348–356.

[7] M.J. Shannag, M.A. Alhassan, Seismic upgrade of interior beam-column sub assemblages with high-performance fiber-reinforced concrete jackets, ACI Struct. J. 102 (1) (2005) 131–138.

[8] G.I. Kalogeropoulos, A.D.G. Tsonos, D. Konstandinidis, S. Tsetines, Pre-earthquake and post-earthquake retrofitting of poorly detailed exterior RC beam-to-column joints, Eng. Struct. 109 (2016) 1–15.

[9] M.N.S. Hadi, T.M. Tran, Retrofitting non-seismically detailed exterior beam-column joints using concrete covers together with CFRP jacket, Constr. Build. Mater. 63 (2014) 161–173.

[10] T. El-Amoury, A. Ghobarah, Seismic rehabilitation of beam–column joint using GFRP sheets, Eng. Struct. 24 (11) (2002) 1397–1407.

[11] A. Prota, A. Nanni, G. Manfredi, E. Cosenza, Selective upgrade of under designed reinforced concrete beam-column joints using carbon fiber-reinforced polymers, ACI Struct. J. 101 (5) (2004) 699–707.

[12] U. Akguzel, S. Pampanin, Recent developments in seismic strengthening of RC beam-column joints with FRP materials, in: Proceedings of the 15th World Conference on Earthquake Engineering, 2012.

[13] H. Sezen, Repair and Strengthening of Reinforced Concrete Beam-Column Joints with Fiber-Reinforced Polymer Composites, J. Compos. Constr. 16 (5) (2012) 499–506.

[14] R. Realfonzo, A. Napoli, J.G.R. Pinilla, Cyclic behavior of RC beam-column joints strengthened with FRP systems, Constr. Build. Mater. 54 (2014) 282–297.

[15] C.D. Vecchio, M.D. Ludovico, A. Prota, G. Manfredi, Analytical model and design approach for FRP strengthening of non-conforming RC corner beam–column joints, Eng. Struct. 87 (2015) 8–20.

[16] Q.S. Yu, S. Noel, C.M. Uang, Experimental Studies on Seismic Rehabilitation of Pre-Northridge Steel Moment Connections: RBS and Haunch Approach, Report No. SSRP-97/09, University of California at San Diego, 1997.

[17] S. Pampanin, C. Christopoulos, Non-invasive retrofit of existing RC frames designed for gravity loads only, in: Proceedings of Concrete Structures in Seismic Regions, 2003.

[18] S. Pampanin, C. Christopoulos, T.H. Chen, Development and validation of a metallic haunch seismic retrofit solution for existing under-designed RC frame buildings, Earthq. Eng. Struct. Dyn. 35 (2006) 1739–1766.

[19] G. Genesio, A. Sharma, R. Eligehausen, S. Pampanin, G.R. Reddy, Development of seismic retrofit technique of RC frame using fully fastened haunch elements: static to dynamic testing, in: Proceedings of 14th Symposium on Earthquake Engineering Indian Institute of Technology, 2010.

[20] A. Sharma, G.R. Reddy, R. Eligehausen, G. Genesio, S. Pampanin, Seismic response of reinforced concrete frames with haunch retrofit solution, ACI Struct. J. 111 (3) (2014) 673–684.

[21] M.K. Sharbatdar, A. Kheyroddin, E. Emami, Cyclic performance of retrofitted reinforced concrete beam–column joints using steel prop, Constr. Build. Mater. 36 (2012) 287–294.

[22] J. Shafaei, A. Hosseini, M.S. Marefat, Seismic retrofit of external RC beam–column joints by joint enlargement using prestressed steel angles, Eng. Struct. 81 (2014) 265–288.

[23] G. Campione, L. Cavaleri, M. Papia, Flexural response of external R.C. beam–column joints externally strengthened with steel cages, Eng. Struct. 104 (2015) 51–64.